Infrared Photodissociation Spectroscopy of $[Mg\cdot(H_2O)_{1-4}]^+$ and $[Mg\cdot(H_2O)_{1-4}\cdot Ar]^+$

Yoshiya Inokuchi,*,†,§ Keijiro Ohshimo,†,|| Fuminori Misaizu,‡ and Nobuyuki Nishi*,†

Institute for Molecular Science, Myodaiji, Okazaki 444-8585, Japan and Department of Chemistry, Tohoku University, Aoba-ku, Sendai 980-8578, Japan

Received: March 25, 2004; In Final Form: April 11, 2004

Infrared photodissociation spectra of $[Mg\cdot(H_2O)_{1-4}]^+$ and $[Mg\cdot(H_2O)_{1-4}\cdot Ar]^+$ are measured in the 3000−3800 cm^{-1} region. For $[Mg\cdot(H_2O)_{1-4}]^+$, cluster geometries are optimized and vibrational frequencies are evaluated by density functional theory calculation. We determine cluster structures of $[Mg\cdot(H_2O)_{1-4}]^+$ by comparison of the infrared photodissociation spectra with infrared spectra calculated for optimized structures of $[Mg\cdot(H_2O)_{1-4}]^+$. In the $[Mg\cdot(H_2O)_{1-3}]^+$ ions, all the water molecules are directly bonded to the Mg^+ ion. The infrared photodissociation spectra of $[Mg\cdot(H_2O)_4]^+$ and $[Mg\cdot(H_2O)_4\cdot Ar]^+$ show bands due to hydrogen-bonded OH stretching vibrations in the 3000−3450 cm^{-1} region. In the $[Mg\cdot(H_2O)_4]^+$ ion, three water molecules are attached to the Mg^+ ion, forming the first solvation shell; the fourth molecule is bonded to the first solvation shell. As a result, the most stable isomer of $[Mg\cdot(H_2O)_4]^+$ has a six-membered ring composed of the Mg^+ ion, two of the three water molecules in the first solvation shell, and a termination water molecule.

1. Introduction

Metal−water cluster ions in the gas phase are microscopic models for fundamental interactions in metal ion hydration. For hydrated magnesium monocations, several experimental[1−10] and theoretical[11−17] studies have been devoted to examining structures and chemical reactions. As for the intermolecular interaction in the ions, Armentrout and co-workers reported binding energies of $[Mg\cdot(H_2O)_{1-4}]^+$ measured by collision-induced dissociation.[7] To investigate intracluster dehydrogenation reactions, the flow tube method[8] and the FT-ICR technique[9,10] were applied to the $[Mg\cdot(H_2O)_n]^+$ ions. Spectroscopically, the photodissociation spectroscopy has been substantially carried out for $[Mg\cdot(H_2O)_n]^+$ in the UV and visible region.[1−6] Photodissociation spectra of the $[Mg\cdot(H_2O)_1]^+$ ion in the 26000−40000 cm^{-1} region show bands due to the $^2P-^2S$ type transitions of Mg^+.[1−5] Duncan and co-workers experimentally demonstrated that the $[Mg\cdot(H_2O)_1]^+$ ion has a geometric structure with C_{2v} symmetry.[3] In the excited $^2B_2$ state of $[Mg\cdot(H_2O)_1]^+$, the symmetric and asymmetric OH stretching vibrations have frequencies of 3360 and 3632 cm^{-1}, respectively.[3] Fuke and co-workers extended the measurement of the electronic spectra of $[Mg\cdot(H_2O)_n]^+$ to $n = 5$.[1,4,5] The $^2P-^2S$ transitions of the Mg^+ chromophore show a significant red-shift from $n = 1$ to $n = 3$. On the other hand, band positions of the $n = 4$ and $n = 5$ ions are almost the same as that of the $n = 3$ ion; the effect of the fourth and fifth water molecules is negligible on the electronic structure of the Mg^+ ion, and the first solvation shell closes at $n = 3$.[4,5] However, the idea of the shell closure in $[Mg\cdot(H_2O)_n]^+$ seems to be still inconclusive, because the bands in the electronic spectra are too broad to obtain vibronic structures and transition energies precisely. Theoretically, ab initio molecular orbital (MO) calculations were done to obtain stable structures, binding energies, and harmonic frequencies of the Mg^+−water clusters.[11−17] Bauschlicher and Partridge[13] and Iwata's group[16] suggested that the first solvation shell consists of three water molecules in the $[Mg\cdot(H_2O)_4]^+$ ion. However, there have been no experimental results that can be directly compared to the theoretical ones to evaluate the validity of the calculations.

As demonstrated in the previous spectroscopic reports,[1−5] electronic spectra provide quite valuable information on electronic structures and ion cores of cluster ions. However, it is difficult to obtain detailed aspects of geometric structures from electronic spectra. Vibrational spectroscopy is one of the most powerful methods to determine structures. In particular, the infrared photodissociation spectroscopy is quite useful for cluster ions.[18−22] By measuring infrared photodissociation spectra, vibrational frequencies are obtained for cluster ions. Cluster structures can be determined by comparison of experimental infrared spectra with theoretical ones for certain structures. With respect to hydrated metal ions, Lisy and co-workers have reported pioneering works of the infrared photodissociation spectroscopy of hydrated alkali metal ions.[23−29] For hydrated systems, OH stretching vibrations emerge in the infrared region of 3000−3800 cm^{-1}. Frequencies and infrared intensities of these vibrations are quite sensitive to the formation of the hydrogen-bond network. In addition, Duncan and co-workers have successfully demonstrated solvation features of CO_2 or H_2O to Fe^+, Mg^+, Al^+, and V^+ with the infrared photodissociation spectroscopy and ab initio MO calculation.[30−34]

In this paper, we report a structural study of $[Mg\cdot(H_2O)_n]^+$ ($n = 1-4$). Infrared photodissociation spectra of $[Mg\cdot(H_2O)_n]^+$ and $[Mg\cdot(H_2O)_n\cdot Ar]^+$ are measured in the 3000−3800 cm^{-1} region by use of an ion guide spectrometer and a pulsed infrared laser. Geometries of the $[Mg\cdot(H_2O)_n]^+$ ions are optimized and vibrational frequencies are evaluated by density functional theory (DFT) calculations. By comparing the experimental spectra with the theoretical ones for the optimized structures, we determine stable structures of $[Mg\cdot(H_2O)_{1-4}]^+$. Hydration features characteristic of the Mg^+ ion are discussed in relation to other hydrated ions.

* To whom correspondence should be addressed. E-mail:ino@ims.ac.jp.
† Institute for Molecular Science.
‡ Tohoku University.
§ Present Address: Department of Basic Science, Graduate School of Arts and Sciences, The University of Tokyo, Komaba, Meguro-ku, Tokyo 153-8902, Japan.
|| Present Address: Chemical Dynamics Laboratory, RIKEN, Wako, Saitama 351-0198, Japan.

10.1021/jp0486752 CCC: $27.50
Published on Web 05/18/2004

2. Experimental and Computational Section

Infrared photodissociation spectra of $[Mg\cdot(H_2O)_n]^+$ and $[Mg\cdot(H_2O)_n\cdot Ar]^+$ ($n = 1-4$) are measured by use of an ion guide spectrometer with two quadrupole mass filters.[35] Cluster ions are produced in a pick-up-type cluster source. Gas mixture of water (~1% content) and argon is introduced into a vacuum chamber through a pulsed nozzle (General Valve model Series 9) with a 0.80-mm orifice diameter, a pulse duration of ~300 μs, and a repetition rate of 10 Hz. The total stagnation pressure is 3×10^5 Pa. Mg^+ ions are produced by laser irradiation of a rotating Mg rod (6-mm diameter) that is located at 5 mm downstream from the exit of the pulsed nozzle. The second harmonic (532 nm, 5 mJ/pulse) of a Nd:YAG laser (Spectra Physics model INDI-50) is focused by a lens with a focal length of 300 mm. Neutral clusters pick up Mg^+ ions, producing hydrated Mg^+ ions. After passing through a skimmer, cluster ions are introduced into the spectrometer with a 50 eV kinetic energy. Parent ions are isolated by the first quadrupole mass filter. After deflection by 90° through an ion bender, parent ions are led into a quadrupole ion guide. The ion beam is merged with a laser beam in the ion guide, and parent ions are excited into vibrationally excited states. The excitation induces fragmentation of parent ions. Resultant fragment ions are mass-analyzed by the second quadrupole mass filter and detected by a secondary electron multiplier tube. For normalization of fragment-ion yields, the power of the dissociation laser is monitored by a pyroelectric detector (Molectron model P1-15H-CC). Both ion signals from the ion detector and laser signals from the pyroelectric detector are fed into a digital storage oscilloscope (LeCroy model 9314A). The oscilloscope is controlled by a microcomputer through the general purpose interface bus (GPIB). Infrared photodissociation spectra of parent ions are obtained by plotting normalized yields of fragment ions against wavenumber of the dissociation laser.

The tunable infrared source used in this study is an optical parametric oscillator (OPO) system (Continuum model Mirage 3000) pumped with an injection-seeded Nd:YAG laser (Continuum model Powerlite 9010). The output energy is 1−2 mJ/pulse, and the line width is approximately 1 cm^{-1}. The infrared light is loosely focused by a CaF_2 lens (a focal length of 1000 mm) located just before the spectrometer. The wavenumber of the OPO laser is calibrated by a commercial wavemeter (Burleigh model WA-4500).

In addition, the $[Mg\cdot(H_2O)_n]^+$ ($n = 1-4$) ions are analyzed by DFT calculations. The calculations are made with the Gaussian 98 program package.[36] Geometry optimization and vibrational frequency evaluation are carried out at the B3LYP/6-31+G* level of theory. For calculated frequencies, we use a scaling factor of 0.9654 for comparison of infrared spectra calculated and experimentally observed.

3. Results and Discussion

A. Infrared Photodissociation Spectra of $[Mg\cdot(H_2O)_n]^+$ and $[Mg\cdot(H_2O)_n\cdot Ar]^+$ ($n = 1-4$). Infrared photodissociation spectra of $[Mg\cdot(H_2O)_n]^+$ ($n = 1-4$) are displayed in Figure 1. The spectra of $[Mg\cdot(H_2O)_n]^+$ are observed by monitoring yields of the fragment $[Mg\cdot(H_2O)_{n-1}]^+$ ions; evaporation of no more than one molecule is seen under our experimental condition. Dissociation is quite inefficient for $[Mg\cdot(H_2O)_{1,2}]^+$; less than 1% of parent ions is dissociated at the maximum. The binding energies of the $n = 1$ and $n = 2$ ions much greater than the infrared photon energies prevent efficient dissociation. Duncan and co-workers reported that the dissociation energy of the $n = 1$ ion is 8514 cm^{-1},[3] and Armentrout's group showed that the bond energies of the $n = 1$ and $n = 2$ ions are 9933 and 7835 cm^{-1}.[7] The $[Mg\cdot(H_2O)_{1,2}]^+$ ions have relatively broad absorption bands that spreads over 3200−3700 cm^{-1}. For the $[Mg\cdot(H_2O)_3]^+$ ion, two bands clearly emerge at 3560 and 3660 cm^{-1}; no band is observed in the 3100−3500 cm^{-1} region. In the spectrum of the $[Mg\cdot(H_2O)_4]^+$ ion, quite broad bands are seen around 3180 and 3370 cm^{-1} in addition to a relatively sharp band at 3650 cm^{-1}.

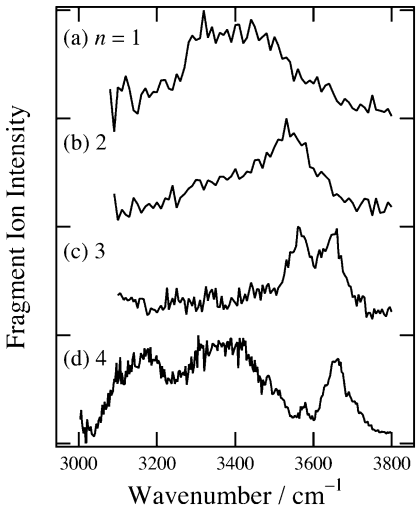

Figure 1. Infrared photodissociation spectra of $[Mg\cdot(H_2O)_n]^+$ ($n = 1-4$). The dissociation pathway monitored for the spectra is loss of one water molecule. All the spectra are normalized by the laser power.

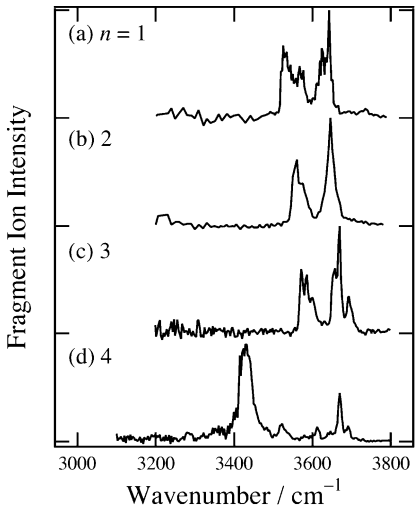

Figure 2. Infrared photodissociation spectra of $[Mg\cdot(H_2O)_n\cdot Ar]^+$ ($n = 1-4$). The dissociation pathway monitored for the spectra is loss of an argon atom. All the spectra are normalized by the laser power.

Figure 2 shows infrared photodissociation spectra for $[Mg\cdot(H_2O)_n\cdot Ar]^+$ ($n = 1-4$) in the $[Mg\cdot(H_2O)_n]^+$ fragment channel. Bandwidths of the spectra are quite narrower than those of $[Mg\cdot(H_2O)_n]^+$. For the $[Mg\cdot(H_2O)_1\cdot Ar]^+$ ion, two bands emerge around 3525 and 3640 cm^{-1}. The $[Mg\cdot(H_2O)_2\cdot Ar]^+$ ion shows two bands at 3560 and 3645 cm^{-1}. The spectrum of the $[Mg\cdot(H_2O)_3\cdot Ar]^+$ ion has two maxima at 3570 and 3670 cm^{-1} with some structures. The $[Mg\cdot(H_2O)_4\cdot Ar]^+$ ion has spectral features different from those of $[Mg\cdot(H_2O)_{1-3}\cdot Ar]^+$; the spectrum displays a strong band at 3429 cm^{-1} and a weak but reproducible band at 3351 cm^{-1} with a few bands in the 3500−3700 cm^{-1} region.

We collect total energies, energies relative to the most stable isomers, and binding energies of optimized structures in Table 1. The structures are shown in the following sections. The

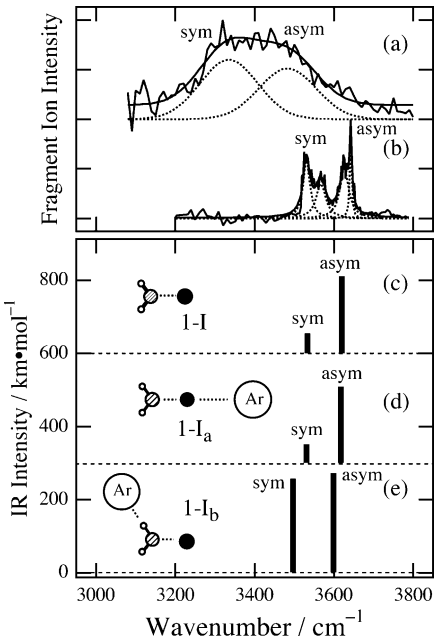

Figure 3. Experimental spectra of (a) $[Mg\cdot(H_2O)_1]^+$ and (b) $[Mg\cdot(H_2O)_1\cdot Ar]^+$. These spectra can be decomposed into a few components (dotted lines). The component positions of $[Mg\cdot(H_2O)_1\cdot Ar]^+$ are 3531, 3567, 3626, and 3642 cm^{-1}. Theoretical spectra obtained from DFT calculations at the B3LYP/6-31+G* level for (c) Form 1-I, (d) Form 1-I$_a$, and (e) Form 1-I$_b$. A scaling factor of 0.9654 is used for the calculated frequencies.

TABLE 1: DFT-Calculated Absolute Energy (E_{zpve}), Relative Energy to the Most Stable Isomers (ΔE), and Binding Energy (E_{bind}) of $[Mg\cdot(H_2O)_n]^+$ ($n = 1-4$)

species	E_{zpve},[a] hartree	ΔE cm^{-1}	E_{bind},[b] cm^{-1}
Mg^+	−199.795513		
H_2O	−76.401473		
1-I	−276.248461		11298
2-I	−352.689992		8792
3-I	−429.125100	0	7382
3-II	−429.120743	956	6426
4-I	−505.551894	0	5557
4-II	−505.550037	408	5150

[a] Corrected with zero-point vibrational energies. [b] $E_{bind}(n) = -E_{zpve}(n) + E_{zpve}(n-1) + E_{zpve}(H_2O)$, where $E_{zpve}(n-1)$ is the energy of the most stable isomer of the $(n-1)$ ion.

binding energies of $[Mg\cdot(H_2O)_n]^+$ are estimated to be much higher than the energy of the infrared laser, and therefore multiphoton processes are necessary for dissociation of cold $[Mg\cdot(H_2O)_n]^+$ clusters. However, multiphoton processes hardly occur in our spectrometer, because the photon density in the ion guide is sparse.[21] The $[Mg\cdot(H_2O)_n]^+$ ions are dissociated through one-photon absorption with the aid of internal energy; the infrared photodissociation spectra of $[Mg\cdot(H_2O)_n]^+$ measured in our experiment are regarded as infrared spectra of "hot" ions. On the other hand, the $[Mg\cdot(H_2O)_n\cdot Ar]^+$ complexes have smaller binding energies; Duncan and co-workers reported that the binding energy of Mg^+-Ar is 1281 cm^{-1}.[37] Therefore, the $[Mg\cdot(H_2O)_n\cdot Ar]^+$ ions located at the vibrationless level can be dissociated through one-photon absorption.

B. The $n = 1$ Ions. Figure 3 shows the infrared photodissociation spectra of $[Mg\cdot(H_2O)_1]^+$ and $[Mg\cdot(H_2O)_1\cdot Ar]^+$ with spectra calculated for minimum-energy structures. For $n = 1$, DFT calculations are carried out also for argon complexes; the structures and the spectra are displayed in Figure 3d and 3e. Form 1-I has a C_{2v} structure, and the distance between the magnesium and oxygen atoms is 2.08 Å. In Form 1-I$_a$, the argon atom is located on the other side of the water molecule. Form 1-I$_b$ has an O−H···Ar intermolecular bond. Form 1-I$_b$ is more stable than Form 1-I$_a$ only by 207 cm^{-1}. For Form 1-I$_a$, the symmetric and asymmetric OH stretching vibrations do not show noticeable change in frequency and infrared intensity from those of Form 1-I. On the other hand, the vibrations of Form 1-I$_b$ show a small shift to the lower frequency by ∼20 cm^{-1} from those of Forms 1-I and 1-I$_a$. As seen in Figure 3b, the spectrum of the $[Mg\cdot(H_2O)_1\cdot Ar]^+$ ion displays two bands around 3525 and 3640 cm^{-1} with some structure. The former band is assigned to the symmetric OH stretching vibration, and it can be divided into two components at 3531 and 3567 cm^{-1}. In $[Cs\cdot(H_2O)_1\cdot Ar]^+$ and $[V\cdot(H_2O)_1\cdot Ar]^+$, the symmetric OH stretch is observed as a single band, whereas the asymmetric one has rotational structures.[26,34] The $[Cs\cdot(H_2O)_1\cdot Ar]^+$ and $[V\cdot(H_2O)_1\cdot Ar]^+$ ions have C_{2v} structures similar to Form 1-I$_a$. The *P* and *R* branches can be observed for the symmetric stretch, because the transition moment is parallel to the symmetry axis and only $\Delta K = 0$ transitions are allowed.[38] Lower internal temperatures of these ions result in the presence of a single band in the symmetric stretch region. For the asymmetric stretch, the vibrational transition moment is perpendicular to the symmetric axis, and the rotational structures of $\Delta K = 1$ transition are observed for the $[Cs\cdot(H_2O)_1\cdot Ar]^+$ and $[V\cdot(H_2O)_1\cdot Ar]^+$ ions.[38] Although the ion source used in this study is not the same as those for the Cs and V systems, the similar tendency that the symmetric stretch appears as a single band should be seen for Form 1-I$_a$. Because Form 1-I$_b$ has the argon atom off the C_2 axis, yielding much smaller rotational constants, Form 1-I$_b$ may also have a symmetric stretch band with no resolved structure. Therefore, the two components in the symmetric stretch region may not be due to a rotational structure of a single isomer. Comparison of the spectra in Figure 3 suggests that the components at 3531 and 3567 cm^{-1} are ascribed to the symmetric OH stretches of Forms 1-I$_b$ and 1-I$_a$, respectively. The coexistence of Forms 1-I$_a$ and 1-I$_b$ should provide two components also in the asymmetric stretch region. The band around 3640 cm^{-1} for $[Mg\cdot(H_2O)_1\cdot Ar]^+$ can be decomposed into two components at 3626 and 3642 cm^{-1}. These components are ascribed to the asymmetric stretches of Forms 1-I$_b$ and 1-I$_a$, respectively. No bands assignable to a rotational structure are observed in the asymmetric stretch region of $[Mg\cdot(H_2O)_1\cdot Ar]^+$. This should be because the position of the argon is quite floppy with an internal temperature higher than those of $[Cs\cdot(H_2O)_1\cdot Ar]^+$ and $[V\cdot(H_2O)_1\cdot Ar]^+$, providing small rotational constants and no resolved structure for $[Mg\cdot(H_2O)_1\cdot Ar]^+$. In addition, the production of a hydroxide species, $[H-Mg-OH]^+$, can be ruled out for the $n = 1$ ion, because the $[Mg\cdot(H_2O)_1\cdot Ar]^+$ ion does not show any noticeable band around 3700 cm^{-1} characteristic of the $[H-Mg-OH]^+$ ion.[35] Our DFT calculations for $n = 1-4$ predict that the change in frequency and infrared intensity between $[Mg\cdot(H_2O)_n]^+$ and $[Mg\cdot(H_2O)_n\cdot Ar]^+$ is largest for $n = 1$. The attached argon atom causes a shift of no more than ∼15 cm^{-1} for $n \geq 2$, even though argon is bound to an OH group. The frequency difference between $[Mg\cdot(H_2O)_n]^+$ and $[Mg\cdot(H_2O)_n\cdot Ar]^+$ is small compared to the difference in band positions between isomers of $[Mg\cdot(H_2O)_n]^+$, as seen in the following sections. Therefore, it is practically reasonable that structures of $[Mg\cdot(H_2O)_n]^+$ are determined by comparison of the experimental spectra of $[Mg\cdot(H_2O)_n\cdot Ar]^+$ with theoretical ones of $[Mg\cdot(H_2O)_n]^+$ for $n \geq 2$.

The experimental spectrum for $[Mg\cdot(H_2O)_1]^+$ consists of two broad components around 3335 and 3485 cm^{-1}. These components can be assigned to the symmetric and asymmetric OH

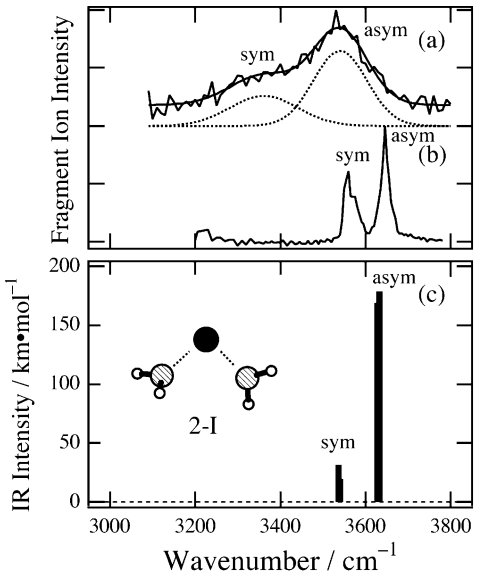

Figure 4. Experimental spectra of (a) $[Mg\cdot(H_2O)_2]^+$ and (b) $[Mg\cdot(H_2O)_2\cdot Ar]^+$. Dotted lines represent components used for the reproduction of the spectrum. (c) Theoretical spectra obtained from DFT calculations at the B3LYP/6-31+G* level for Form 2-I.

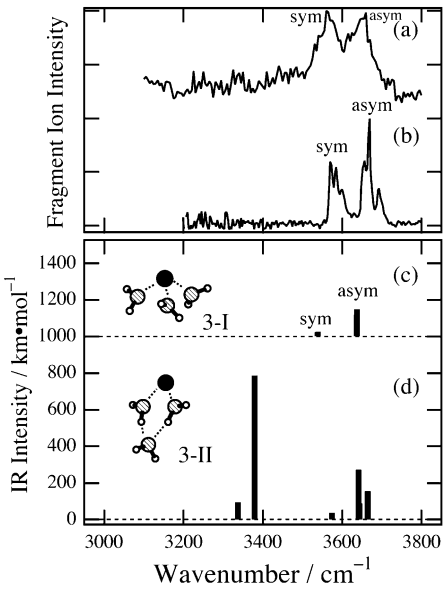

Figure 5. Experimental spectra of (a) $[Mg\cdot(H_2O)_3]^+$ and (b) $[Mg\cdot(H_2O)_3\cdot Ar]^+$. Theoretical spectra obtained from DFT calculations at the B3LYP/6-31+G* level for (c) Form 3-I and (d) Form 3-II.

stretching vibrations, although they show a fairly large shift to the lower frequency from those of the cold ($[Mg\cdot(H_2O)_1\cdot Ar]^+$) ion. The shift may be due to the anharmonic coupling of the OH stretches with the bath of low-frequency modes. As mentioned above, the infrared photodissociation spectrum of the $[Mg\cdot(H_2O)_1]^+$ ion measured in this study is considered as an infrared spectrum of "hot" ions. Therefore, the bands observed in the spectrum of $[Mg\cdot(H_2O)_1]^+$ are ascribed to the transition from (0, *N*) to (1, *N*) states, where the first index stands for the vibrational quantum numbers of the OH stretches, and the second one (*N*) represents the summation of vibrational quantum numbers of low-frequency modes. The anharmonic coupling causes decrease in the energy spacing between the (0, *N*) and (1, *N*) states compared to that between the (0, 0) and (1, 0) states.[39,40]

C. The $n = 2$ and $n = 3$ Ions. Figure 4 exhibits the infrared photodissociation spectra of $[Mg\cdot(H_2O)_2]^+$ and $[Mg\cdot(H_2O)_2\cdot Ar]^+$ with a spectrum calculated for Form 2-I. In Form 2-I, both water molecules are directly solvated to the Mg^+ ion. The absorption of $[Mg\cdot(H_2O)_2]^+$ (Figure 4a) is composed of two broad components around 3360 and 3540 cm^{-1}. In the spectrum of $[Mg\cdot(H_2O)_2\cdot Ar]^+$ (Figure 4b), two sharp bands emerge at 3560 and 3645 cm^{-1}. These bands of $[Mg\cdot(H_2O)_2]^+$ and $[Mg\cdot(H_2O)_2\cdot Ar]^+$ are assigned to the symmetric and asymmetric OH stretching vibrations of the water molecules. The spectrum calculated for Form 2-I (Figure 4c) well reproduces the observed spectrum of $[Mg\cdot(H_2O)_2\cdot Ar]^+$. Therefore, the structure of the $[Mg\cdot(H_2O)_2]^+$ ion is attributed to a symmetric one like Form 2-I.

The infrared photodissociation spectra of $[Mg\cdot(H_2O)_3]^+$ and $[Mg\cdot(H_2O)_3\cdot Ar]^+$ are compared with calculated spectra in Figure 5. In Form 3-I, all the water molecules are directly attached to the Mg^+ ion. Form 3-II has two hydrogen bonds, forming a ring structure. Spectral features of $[Mg\cdot(H_2O)_3]^+$ and $[Mg\cdot(H_2O)_3\cdot Ar]^+$ are similar to each other. In the observed spectrum of $[Mg\cdot(H_2O)_3]^+$ (Figure 5a), two bands appear at 3560 and 3660 cm^{-1}. The experimental spectrum of $[Mg\cdot(H_2O)_3\cdot Ar]^+$ (Figure 5b) displays two maxima at 3570 and 3670 cm^{-1}. Since both spectra show no band in the hydrogen-bonded OH stretching region, there is no water−water intermolecular bond in the $n = 3$ ions. This experimental result excludes the possibility of the formation of Form 3-II. Form 3-I has the symmetric OH stretching vibrations of the water molecules at 3537, 3538, and 3539 cm^{-1}, and the asymmetric ones at 3636, 3637, and 3637 cm^{-1}. Therefore, the two maxima in the experimental spectra of $[Mg\cdot(H_2O)_3]^+$ and $[Mg\cdot(H_2O)_3\cdot Ar]^+$ correspond to the symmetric and asymmetric OH stretches of the water molecules; the structure of $[Mg\cdot(H_2O)_3]^+$ is Form 3-I. In the spectrum of $[Mg\cdot(H_2O)_3\cdot Ar]^+$, several subbands are also seen in the 3500−3700 cm^{-1} region. These bands may be due to combination bands involving intermolecular vibrations or structural isomers with different positions of Ar. In any case, however, it is unambiguous that the partial structure of $[Mg\cdot(H_2O)_3]^+$ in $[Mg\cdot(H_2O)_3\cdot Ar]^+$ is almost the same as Form 3-I.

In Forms 2-I and 3-I, the water molecules are located on the same side of the Mg^+ ion. These structures are due to the polarization of the Mg^+ 3s orbital. The solvation of the first water molecule creates a region of high electron density on the backside of the ion. The second and the third water molecules are solvated on the same side of the first molecule, avoiding the region of high electron density. The similar structures were theoretically proposed in several papers.[12,13,15,16]

D. The $n = 4$ Ions. Figure 6 displays the infrared photodissociation spectra of $[Mg\cdot(H_2O)_4]^+$ (Figure 6a) and $[Mg\cdot(H_2O)_4\cdot Ar]^+$ (Figure 6b) and infrared spectra calculated for Forms 4-I and 4-II (Figure 6c and 6d). The observed spectrum of $[Mg\cdot(H_2O)_4]^+$ shows two broad bands around 3180 and 3370 cm^{-1}. The $[Mg\cdot(H_2O)_4\cdot Ar]^+$ ion has a strong band at 3429 cm^{-1} and a weak but reproducible band at 3351 cm^{-1}. These bands in the 3000−3450 cm^{-1} region can be ascribed to hydrogen-bonded OH stretches. The calculated spectra show hydrogen-bonded OH stretching vibrations in the same region; the positions of these bands are characteristic of the forms. In Form 4-I, three water molecules are directly connected to the Mg^+ ion; two of the three molecules are involved in a six-membered ring. The hydrogen-bonded OH oscillators show one strong band at 3407 cm^{-1} and a weak one at 3373 cm^{-1}. Form 4-II has a hydrogen-bonded OH stretch at 3165 cm^{-1}; the frequency is lower than those of Form 4-I. Comparison of the spectra observed and calculated implies that the broad bands around 3180 and 3370 cm^{-1} in the experimental spectrum of $[Mg\cdot(H_2O)_4]^+$ can be attributed to Forms 4-II and 4-I, respec-

TABLE 2: Observed and Calculated Frequencies and Assignment of the Infrared Spectra of $[Mg\cdot(H_2O)_n]^+$ and $[Mg\cdot(H_2O)_n\cdot Ar]^+$ ($n = 1-4$)

observed frequency cm^{-1}				
$[Mg(H_2O)_n]^+$	$[Mg(H_2O)_n\cdot Ar]^+$	calculated frequency,[a] cm^{-1}	form	assignment[b]
		$n = 1$		
3335	3531	3497 (257)	1-I_b	sym. OH
	3567	3530 (52)	1-I_a	
3485	3626	3599 (273)	1-I_b	asym. OH
	3642	3618 (209)	1-I_a	
		$n = 2$		
3360	3560	3537 (32), 3540 (20)	2-I	sym. OH
3540	3645	3629 (169), 3633 (179)	2-I	asym. OH
		$n = 3$		
3560	3570	3537 (17), 3538 (24), 3539 (24)	3-I	sym. OH
3660	3670	3636 (118), 3637 (149), 3637 (149)	3-I	asym. OH
		$n = 4$		
3180		3165 (1219)	4-II	H-bonded OH
3370	3351	3373 (79)	4-I	H-bonded OH
	3429	3407 (600)	4-I	H-bonded OH
3483	3522	3533 (12)	4-I	sym. OH
3576	3612	3578 (23)	4-I	sym. OH of 2°
3632	3644	3643 (161)	4-I	asym. OH
3658	3669	3640 (179), 3641 (85)	4-I	free OH
3688	3691	3672 (142)	4-I	asym. OH of 2°

[a] A scaling factor of 0.9654 is used for the calculated frequencies. Values in the parentheses are infrared intensities in $km\cdot mol^{-1}$. [b] 2° stands for a water molecule located in the second solvation shell.

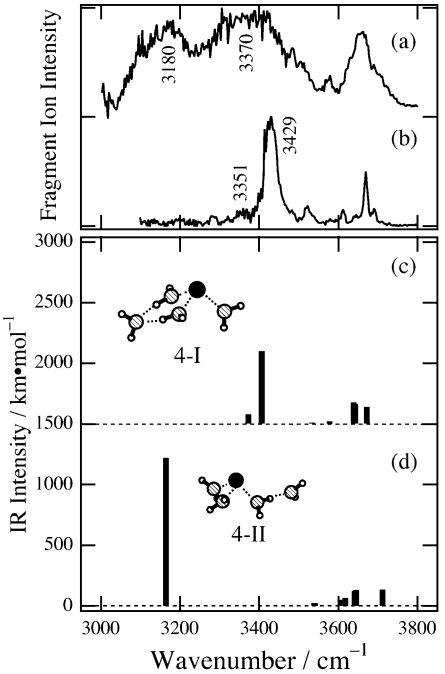

Figure 6. Experimental spectra of (a) $[Mg\cdot(H_2O)_4]^+$ and (b) $[Mg\cdot(H_2O)_4\cdot Ar]^+$. Theoretical spectra obtained from DFT calculations at the B3LYP/6-31+G* level for (c) Form 4-I and (d) Form 4-II.

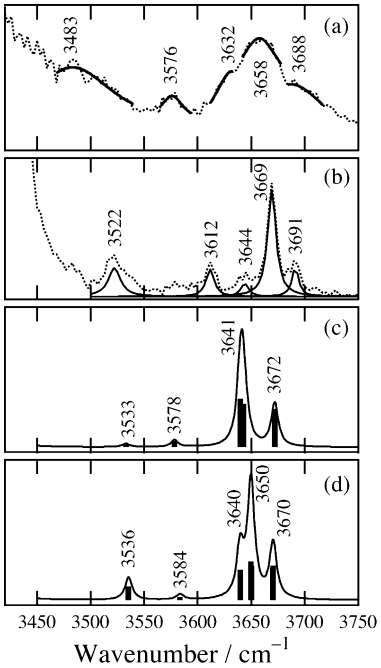

Figure 7. Enlarged view of the observed and calculated spectra of the $n = 4$ ions in the 3450−3750 cm^{-1} region. (a, b) Experimental spectra of $[Mg\cdot(H_2O)_4]^+$ and $[Mg\cdot(H_2O)_4\cdot Ar]^+$ (dotted lines). Solid lines in Figure 7a highlight humps of the spectrum. Solid lines in Figure 7b represent Lorentzian functions used for the reproduction of the observed spectrum. (c) Theoretical spectrum of Form 4-I with the 6-31+G* basis set. (d) Theoretical spectrum of Form 4-I with the 6-311+G* basis set. Solid curves in Figure 7c and 7d represent convolution of the stick spectra by Lorentzian functions with a width of 8 cm^{-1} (fwhm).

tively. The 3370-cm^{-1} component is observed almost two times stronger than the 3180-cm^{-1} component. In contrast, the infrared intensity of the hydrogen-bonded OH bands for Form 4-I relative to that for Form 4-II is $(79 + 600)/1219 = \sim 0.6$. From these quantities, we can roughly estimate the relative abundance of Forms 4-I and 4-II as 1:0.3. For $[Mg\cdot(H_2O)_4\cdot Ar]^+$, the internal temperature lower than that of $[Mg\cdot(H_2O)_4]^+$ should provide mainly the most stable isomer. Since the band position and the relative intensity of the hydrogen-bonded OH stretches of $[Mg\cdot(H_2O)_4\cdot Ar]^+$ are fairly coincident with those of Form 4-I, the $[Mg\cdot(H_2O)_4\cdot Ar]^+$ ion produced in our experiment has a partial structure of Form 4-I. Therefore, these experimental results of the $n = 4$ ions verify that the most stable structure of $[Mg\cdot(H_2O)_4]^+$ is Form 4-I. This conclusion is consistent with the theoretical result that Form 4-I is the most stable in our DFT calculations.

Evidence of the preference of Form 4-I is also seen in the 3450−3750 cm^{-1} region. Expanded view of the spectra in the 3450−3750 cm^{-1} region is shown in Figure 7. In $[Mg\cdot(H_2O)_4\cdot Ar]^+$, five bands clearly appear at 3522, 3612, 3644, 3669, and 3691 cm^{-1}. In the observed spectrum of $[Mg\cdot(H_2O)_4]^+$,

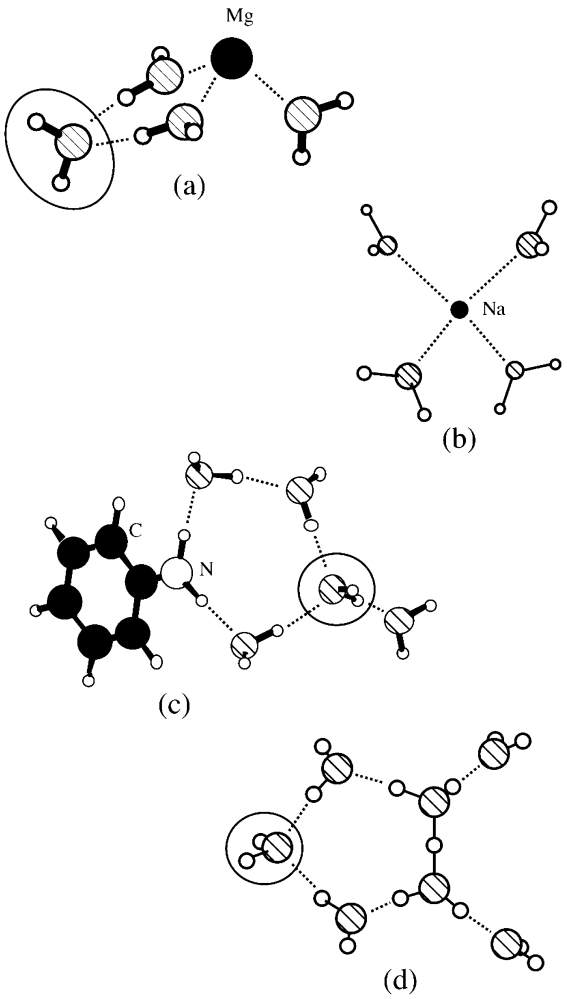

Figure 8. Structures of hydrated ions: (a) $[Mg\cdot(H_2O)_4]^+$, (b) $[Na\cdot(H_2O)_4]^+$, (c) $[aniline\cdot(H_2O)_5]^+$, and (d) $[H\cdot(H_2O)_7]^+$. The isomers in Figure 8b−8d were predicted to be located at the global minima in the previous reports (refs 22 and 42−44). Constituents in the circles of Figure 8a, 8c, and 8d are terminal water molecules, which accept two hydrogen bonds and close a ring.

five humps can be seen at 3483, 3576, 3632, 3658, and 3688 cm^{-1}. These humps may correspond to the bands of $[Mg\cdot(H_2O)_4\cdot Ar]^+$, while the hump positions shift to the lower frequency because of the temperature effect. Figure 7c shows the theoretical spectrum of Form 4-I; the solid line represents a band shape produced on the basis of the Lorentzian band contour (a fwhm of 8 cm^{-1}) for each vibration. The band shape is similar to the observed spectrum of $[Mg\cdot(H_2O)_4\cdot Ar]^+$; the maxima at 3533, 3578, 3641, and 3672 cm^{-1} in Figure 7c correspond to the bands observed at 3522, 3612, 3669, and 3691 cm^{-1} in Figure 7b, respectively. The lack of the observed 3644-cm^{-1} band in the calculated spectrum is solved by the introduction of the 6-311+G* basis set to DFT calculation (B3LYP/6-311+G*). As shown in Figure 7d, the vibrational estimation with the 6-311+G* set decomposes the band predicted at 3641 cm^{-1} with the 6-31+G* set into two maxima at 3640 and 3650 cm^{-1}, which resemble the bands observed at 3644 and 3669 cm^{-1} in Figure 7b.[41] The observed bands in Figure 7b are assigned on the basis of the vibrational analysis with the 6-311+G* basis set and are listed down in Table 2.

E. Comparison of Hydration Structures. The structural features characteristic of the hydrated Mg^+ ions are originated from the occupation of one valence electron in the 3s orbital of the Mg^+ ion. Figure 8 shows structures of four different types of hydrated ions. The $[Mg\cdot(H_2O)_4]^+$ ion has the first solvation shell formed by three water molecules. As described above, the hydration induces the polarization of the Mg^+ 3s orbital. The 3s and 3p orbitals are mixed to each other to produce sp^3-like hybridization. The valence electron is located at one of the hybrid molecular orbitals, and the three water molecules are led to the other three orbitals. As a result, all the water molecules are on the same side of the Mg^+ ion, and the first solvation shell closes with three water molecules. Figure 8b displays the structure of $[Na\cdot(H_2O)_4]^+$ that was theoretically the most stable.[42,43] The hydration shell of Na^+ was experimentally determined to be four by infrared spectroscopy, although hexacoordinated Na^+ cluster ions were also found in the gas phase.[27] The tetrahedral structure of $[Na\cdot(H_2O)_4]^+$ and the large flexibility of the solvation number of Na^+ probably come from the $(3s)^0$ closed-shell structure and the spherical charge distribution of Na^+.

As shown in Figure 8a, the $[Mg\cdot(H_2O)_4]^+$ ion has a six-membered ring. Figure 8c and 8d displays the structures of $[aniline\cdot(H_2O)_5]^+$ and $[H\cdot(H_2O)_7]^+$.[22,44] For $aniline^+$ and hydronium ion, at least 10 members are needed to form a cyclic structure, whereas six atoms can produce a ring in the Mg^+ ion. We suppose that the smaller number of the Mg^+ system is also attributed to the electronic structure of the Mg^+ ion. For the formation of a ring structure in cluster ions, a water molecule that terminates a ring on the opposite side of ions is needed as seen in Figure 8a, 8c, and 8d. The termination water is quite unstable, because this molecule has to accept two hydrogen bonds at one oxygen atom. In the hydrated Mg^+ ion, the water molecules are tightly bonded to the highly polarized 3s orbital of Mg^+. The electron density of the water molecules becomes fairly lower than those of free water, $[aniline\cdot(H_2O)_5]^+$, and $[H\cdot(H_2O)_7]^+$, making the effective dipole moment of the OH groups much smaller.[45] As a result, the water molecules in the first solvation shell can be connected to one oxygen atom of a terminal water molecule and form the six-membered ring against structural constraint.

4. Conclusion

We have investigated the structures of the hydrated Mg^+ ions, $[Mg\cdot(H_2O)_{1-4}]^+$. The infrared photodissociation spectra of $[Mg\cdot(H_2O)_{1-4}]^+$ have broad bands due to the temperature effect. On the other hand, the infrared photodissociation spectra of the $[Mg\cdot(H_2O)_{1-4}\cdot Ar]^+$ ions show bands quite sharper than those of the $[Mg\cdot(H_2O)_{1-4}]^+$ ions. We compare the experimental spectra of $[Mg\cdot(H_2O)_{1-4}\cdot Ar]^+$ with the theoretical ones of $[Mg\cdot(H_2O)_{1-4}]^+$ to determine the stable structures of $[Mg\cdot(H_2O)_{1-4}]^+$. In the $[Mg\cdot(H_2O)_{1-3}]^+$ ions, all the water molecules are directly attached to the Mg^+ ion. On the other hand, the $[Mg\cdot(H_2O)_4]^+$ ion has water−water hydrogen bonds. In the most stable structure of $[Mg\cdot(H_2O)_4]^+$, three water molecules are directly solvated to the Mg^+ ion; two of the three molecules are involved in the ring structure with the Mg^+ ion and the fourth water molecule. The hydration number is undoubtedly determined to be three for the singly charged magnesium ion.

References and Notes

(1) Misaizu, F.; Sanekata, M.; Tsukamoto, K.; Fuke, K.; Iwata, S. *J. Phys. Chem.* **1992**, *96*, 8259.

(2) Yeh, C. S.; Willey, K. F.; Robbins, D. L.; Pilgrim, J. S.; Duncan, M. A. *Chem. Phys. Lett.* **1992**, *196*, 233.

(3) Willey, K. F.; Yeh, C. S.; Robbins, D. L.; Pilgrim, J. S.; Duncan, M. A. *J. Chem. Phys.* **1992**, *97*, 8886.

(4) Fuke, K.; Misaizu, F.; Sanekata, M.; Tsukamoto, K.; Iwata, S. *Z. Phys. D* **1993**, *26*, S180.

(5) Misaizu, F.; Sanekata, M.; Fuke, K.; Iwata, S. *J. Chem. Phys.* **1994**, *100*, 1161.
(6) Sanekata, M.; Misaizu, F.; Fuke, K.; Iwata, S.; Hashimoto, K. *J. Am. Chem. Soc.* **1995**, *117*, 747.
(7) Dalleska, N. F.; Tjelta, B. L.; Armentrout, P. B. *J. Phys. Chem.* **1994**, *98*, 4191.
(8) Harms, A. C.; Khanna, S. N.; Chen, B.; Castleman, A. W., Jr. *J. Chem. Phys.* **1994**, *100*, 3540.
(9) Berg, C.; Achatz, U.; Beyer, M.; Joos, S.; Albert, G.; Schindler, T.; Niedner-Schatteburg, G.; Bondybey, V. E. *Int. J. Mass Spectrom. Ion Processes* **1997**, *167*/*168*, 723.
(10) Berg, C.; Beyer, M.; Achatz, U.; Joos, S.; Niedner-Schatteburg, G.; Bondybey, V. E. *Chem. Phys.* **1998**, *239*, 379.
(11) Bauschlicher, C. W., Jr.; Partridge, H. *Chem. Phys. Lett.* **1991**, *181*, 129.
(12) Bauschlicher, C. W., Jr.; Partridge, H. *J. Phys. Chem.* **1991**, *95*, 3946.
(13) Bauschlicher, C. W., Jr.; Partridge, H. *J. Phys. Chem.* **1991**, *95*, 9694.
(14) Sodupe, M.; Bauschlicher, C. W., Jr. *Chem. Phys. Lett.* **1992**, *195*, 494.
(15) Bauschlicher, C. W., Jr.; Sodupe, M.; Partridge, H. *J. Chem. Phys.* **1992**, *96*, 4453.
(16) Watanabe, H.; Iwata, S.; Hashimoto, K.; Misaizu, F.; Fuke, K. *J. Am. Chem. Soc.* **1995**, *117*, 755.
(17) Asada, T.; Iwata, S. *Chem. Phys. Lett.* **1996**, *260*, 1.
(18) Yeh, L. I.; Okumura, M.; Myers, J. D.; Price, J. M.; Lee, Y. T. *J. Chem. Phys.* **1989**, *91*, 7319.
(19) Bieske, E. J.; Maier, J. P. *Chem. Rev.* **1993**, *93*, 2603.
(20) Lisy, J. M. *Cluster Ions*; Wiley: Chichester, U.K., 1993; p 217.
(21) Inokuchi, Y.; Nishi, N. *J. Chem. Phys.* **2001**, *114*, 7059.
(22) Inokuchi, Y.; Ohashi, K.; Honkawa, Y.; Yamamoto, N.; Sekiya, H.; Nishi, N. *J. Phys. Chem. A* **2003**, *107*, 4230.
(23) Weinheimer, C. J.; Lisy, J. M. *J. Chem. Phys.* **1996**, *105*, 2938.
(24) Cabarcos, O. M.; Weinheimer, C. J.; Lisy, J. M. *J. Chem. Phys.* **1998**, *108*, 5151.
(25) Cabarcos, O. M.; Weinheimer, C. J.; Lisy, J. M. *J. Chem. Phys.* **1999**, *110*, 8429.
(26) Vaden, T. D.; Forinash, B.; Lisy, J. M. *J. Chem. Phys.* **2002**, *117*, 4628.
(27) Patwari, G. N.; Lisy, J. M. *J. Chem. Phys.* **2003**, *118*, 8555.
(28) Patwari, G. N.; Lisy, J. M. *J. Phys. Chem. A* **2003**, *107*, 9495.
(29) Vaden, T. D.; Lisy, J. M. *J. Chem. Phys.* **2004**, *120*, 721.
(30) Gregoire, G.; Velasquez, J.; Duncan, M. A. *Chem. Phys. Lett.* **2001**, *349*, 451.
(31) Gregoire, G.; Duncan, M. A. *J. Chem. Phys.* **2002**, *117*, 2120.
(32) Gregoire, G.; Brinkmann, N. R.; van Heijnsbergen, D.; Schaefer, H. F.; Duncan, M. A. *J. Phys. Chem. A* **2003**, *107*, 218.
(33) Walters, R. S.; Brinkmann, N. R.; Schaefer, H. F.; Duncan, M. A. *J. Phys. Chem. A* **2003**, *107*, 7396.
(34) Walker, N. R.; Walters, R. S.; Pillai, E. D.; Duncan, M. A. *J. Chem. Phys.* **2003**, *119*, 10471.
(35) Inokuchi, Y.; Ohshimo, K.; Misaizu, F.; Nishi, N. *Chem. Phys. Lett.* **2004**, *390*, 140.
(36) Frisch, M. J.; Trucks, G. W.; Schlegel, H. B.; Scuseria, G. E.; Robb, M. A.; Cheeseman, J. R.; Zakrzewski, V. G.; Montgomery, Jr., J. A.; Stratmann, R. E.; Burant, J. C.; Dapprich, S.; Millam, J. M.; Daniels, A. D.; Kudin, K. N.; Strain, M. C.; Farkas, O.; Tomasi, J.; Barone, V.; Cossi, M.; Cammi, R.; Mennucci, B.; Pomelli, C.; Adamo, C.; Clifford, S.; Ochterski, J.; Petersson, G. A.; Ayala, P. Y.; Cui, Q.; Morokuma, K.; Malick, D. K.; Rabuck, A. D.; Raghavachari, K.; Foresman, J. B.; Cioslowski, J.; Ortiz, J. V.; Baboul, A. G.; Stefanov, B. B.; Liu, G.; Liashenko, A.; Piskorz, P.; Komaromi, I.; Gomperts, R.; Martin, R. L.; Fox, D. J.; Keith, T.; Al-Laham, M. A.; Peng, C. Y.; Nanayakkara, A.; Challacombe, M.; Gill, P. M. W.; Johnson, B.; Chen, W.; Wong, M. W.; Andres, J. L.; Gonzalez, C.; Head-Gordon, M.; Replogle, E. S.; Pople, J. A. *Gaussian 98 Revision A.9*, Gaussian, Inc.: Pittsburgh, PA, 1998.
(37) Pilgrim, J. S.; Yeh, C. S.; Berry, K. R.; Duncan, M. A. *J. Chem. Phys.* **1994**, *100*, 7945.
(38) Herzberg, G. *Molecular Spectra and Molecular Structure II*; Krieger: Malabar, FL, 1991; p 414.
(39) Nakabayashi, T.; Kamo, S.; Sakuragi, H.; Nishi, N. *J. Phys. Chem. A* **2001**, *105*, 8605.
(40) Asher, S. A.; Murtaugh, J. *J. Am. Chem. Soc.* **1983**, *105*, 7244.
(41) We use a scaling factor of 0.9550 for the frequencies calculated at the B3LYP/6-311+G* level of theory.
(42) Kim, J.; Lee, S.; Cho, S. J.; Mhin, B. J.; Kim, K. S. *J. Chem. Phys.* **1995**, *102*, 839.
(43) Hartke, B.; Charvat, A.; Reich, M.; Abel, B. *J. Chem. Phys.* **2002**, *116*, 3588.
(44) Jiang, J.-C.; Wang, Y.-S.; Chang, H.-C.; Lin, S. H.; Lee, Y. T.; Niedner-Schatteburg, G.; Chang, H.-C. *J. Am. Chem. Soc.* **2000**, *122*, 1398.
(45) This can be confirmed by the reduction of the OH frequencies of $[Mg\cdot(H_2O)_1]^+$ (3525 and 3640 cm^{-1}, this study) from those of $[aniline\cdot(H_2O)_1]^+$ (3628 and 3715 cm^{-1}, see ref 22).